Korean J. Chem. Eng., **28**(8), 1713-1720 (2011)
DOI: 10.1007/s11814-011-0162-x

Destruction of anthracene using a gliding arc plasma reformer

Young Nam Chun*,†, Seong Cheon Kim*, and Kunio Yoshikawa**

*BK21 Team for Hydrogen Production · Department of Environmental Engineering,
Chosun University, 375 Seoseok-dong, Dong-gu, Gwangju 501-759, Korea
*Frontier Research Center, Tokyo Institute of Technology G5-8, 4259 Nagatsuta, Midori-ku, Yokohama 226-8502, Japan
(*Received 5 February 2011 • accepted 21 June 2011*)

Abstract−The gasification technology for biomass conversion has a limitation for some applications, including engines and turbines, because it produces tar-containing gas. In this study, a gliding arc plasma reformer was developed to remove tar. The plasma discharge in the gliding-type reformer is based on the both non-equilibrium and equilibrium plasmas. A simulation test was conducted using anthracene, which is produced during the gasification of biomass and waste, as the representative tar substance. In the optimal condition, the anthracene decomposition efficiency was 96.1%, and the energy efficiency was 1.14 g/kWh. The higher heating value of the gas produced from the anthracene decomposition was 11,324 kJ/Nm^3, and the carbon balance was 98%. The steam flow rate, power input, total gas flow rate, and input concentration change were used as variables for the test. The anthracene decomposition efficiency was 81% when the gliding arc plasma reformer was used. When steam was fed at a rate of 0.63 L/min, the decomposition efficiency was highest (96.1%) due to the creation of OH radicals. The energy efficiency was highest (2.63 g/kWh) when the total gas flow rate was 24.1 L/min. H_2, CO, and CO_2 were produced as reformed gases. At the steam injection rate of 0.37 L/min or more, carbon black did not appear. Thus, it was verified that the gliding arc plasma reformer is effective for tar reduction.

Key words: Tar Decomposition, Gliding Arc Plasma, Anthracene, Reformer, Gasification

INTRODUCTION

The demand for oil is skyrocketing along with its price, and the sense of crisis due to the exhaustion of fossil fuels, environmental pollution, and global warming is growing and has led to the enforcement of the Kyoto Protocol. Accordingly, many studies on diverse new and renewable energy sources are being conducted. However, energy sources like solar energy, wind power, etc., have limitations in terms of their inherent limits and energy efficiency. Therefore, it is essential to convert biomass and waste resources into renewable energy sources. In this regard, the gasification technology is drawing attention because it is the thermochemical conversion method for biomass and waste resources [1-3]. The gasification technology is being used to convert biomass and waste resources into synthetic gas, which has diverse applications, such as in gas turbines, engines, fuel cells, and methanol production [4]. Steam gasification, however, generates tar, which is a mixture of compounds containing polyaromatic hydrocarbons and oxygenates. Condensed at a low temperature, tar causes clogging and corrosion in the pipeline during gasification, and also leads to operation trouble and damage to equipment during the following process, as in gas turbines and engines [3-5]. Accordingly, many studies are under way to remove the tar produced during gasification.

The method of thermal cracking [6,7] or catalytic cracking [8-10] is being studied by many researchers as part of the tar removal technology. For thermal cracking, however, high temperature and sufficient retention time are required. In catalyst tar cracking, the catalysts are sensitive to contaminants such as sulfur, chlorine, and nitrogen compounds, generating in gasification of biomass.

Other than these methods, plasma is also used to remove tar. A number of studies on plasma discharge types, oxidizer types (air, oxygen, etc.), and tar ingredients have been conducted [11,12] as well as studies on the use of adsorption and the wet-type scrubber for tar removal [13-15].

The gliding arc plasma used in this study is advantageous in that it is compact and starts and responds quickly, it can use diverse fuels and biogases containing hydrocarbon polymer for the tar content, and it can ensure optimal operation with a high conversion rate [16].

The gliding arc plasma discharge can be divided in following three phases as shown Fig. 1; (A) reagent gas break-down, (B) equilibrium heating phase, (C) non-equilibrium reaction phase [17]. The initial break-down (A) of the processed gas begins the cycle of the gliding arc evolution. The high voltage generator provides the necessary electric field to break down the gas between the electrodes, and the discharge starts at the shortest distance between the two electrodes. The equilibrium stage (B) takes place after formation of a stable plasma channel. The gas flow convects the resulting small equilibrium plasma volume with a velocity of about 10 m/s, and the length of the arc column increases together with the voltage. The non-equilibrium stage (C) begins when the length of the gliding arc exceeds its critical value. Heat losses from the plasma column begin to exceed the energy supplied by the source, and it is not possible to sustain the plasma in the state of thermodynamic equilibrium. After the decay of the non-equilibrium discharge, there is new break-down at the shortest distance between electrodes and the cycle re-

†To whom correspondence should be addressed.
E-mail: ynchun@chosun.ac.kr

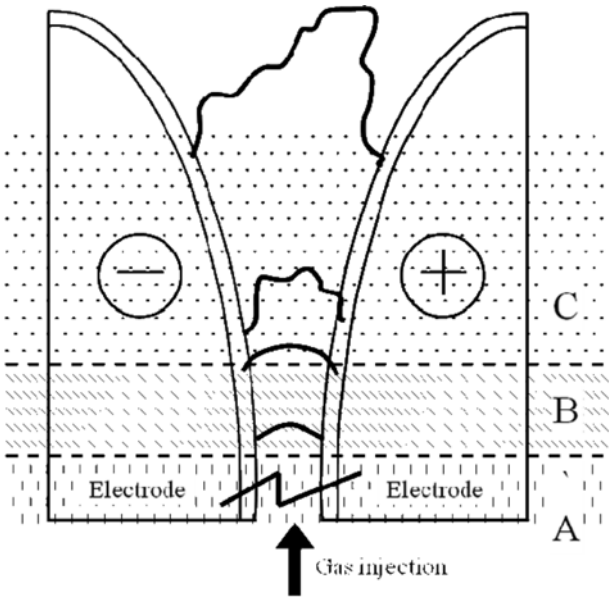

Fig. 1. Phases of gliding arc evolution: (A) reagent gas break-down; (B) Equilibrium heating phase; (C) non-equilibrium reaction phase.

peats. Tar in the plasma arc discharge should be decomposed by cracking and carbon formation reactions (Eqs. (7) and (8)).

In this study, a gliding arc plasma reactor was designed and manufactured to reduce the tar using the plasma technology. Anthracene was selected as the representative substance in the tar content. The experiments were conducted, with the steam flow rate, input power, total gas flow rate, and input concentration change as variables, to identify the tar removal efficiency, reformed-gas concentration and energy efficiency.

TEST EQUIPMENT AND RESEARCH METHOD

1. Test Equipment and Composition

Fig. 2 shows the diagram of the test equipment for the gliding arc plasma reformer that was used for the tar removal test. The equipment consisted of a gliding arc plasma reformer, a steam feeding line, a tar feeding line, a power supply equipment, a measurement and analysis line, and a control and monitoring system.

The gliding arc plasma reactor had three blade-type electrodes (2 mm wide, 95 mm long, and 2 mm thick) mounted with 120 degree, with the center of the reactor as the reference point. The gap between the electrodes was kept constant at 3 mm. Ceramic material (Al_2O_3, 96 wt%) was used to ensure insulation and to fix the electrodes in the reactor. The diameter of the gas nozzle was 1.5 mm. The outer cylinder of the plasma reactor was a quartz tube (55 mm in diameter and 200 mm long) so that insulation could be ensured and the inside could be checked.

The steam feeding line consisted of a steam generator and a water pump (STEPDOS 03 model, KNF, Switzerland). The water tank was filled with distilled water, which was fed into the steam generator by the water pump. The amount of steam was controlled by adjusting the water flow rate using the water pump. The tar feeding line consisted of a mass flow controller (MFC) for controlling the flow rate of dilution nitrogen (F201AC-FAC-22-V model, BRONKHOST, Netherlands), another MFC for controlling the flow rate of nitrogen for tar gas generation (M3030V model, LINETECH, South Korea), and a tar generator. The tar generator consisted of a mantle heater and a tar container. The amount of tar generation was controlled by adjusting the flow rate of nitrogen for tar gas generation.

The power supply equipment consisted of a power supply (UAP-15K1A model, Unicon Tech., South Korea) for supplying high voltage power, and a high-voltage probe, a low-current probe (A6303 model, Tektronix, USA) and an oscilloscope (TDS-3052 model,

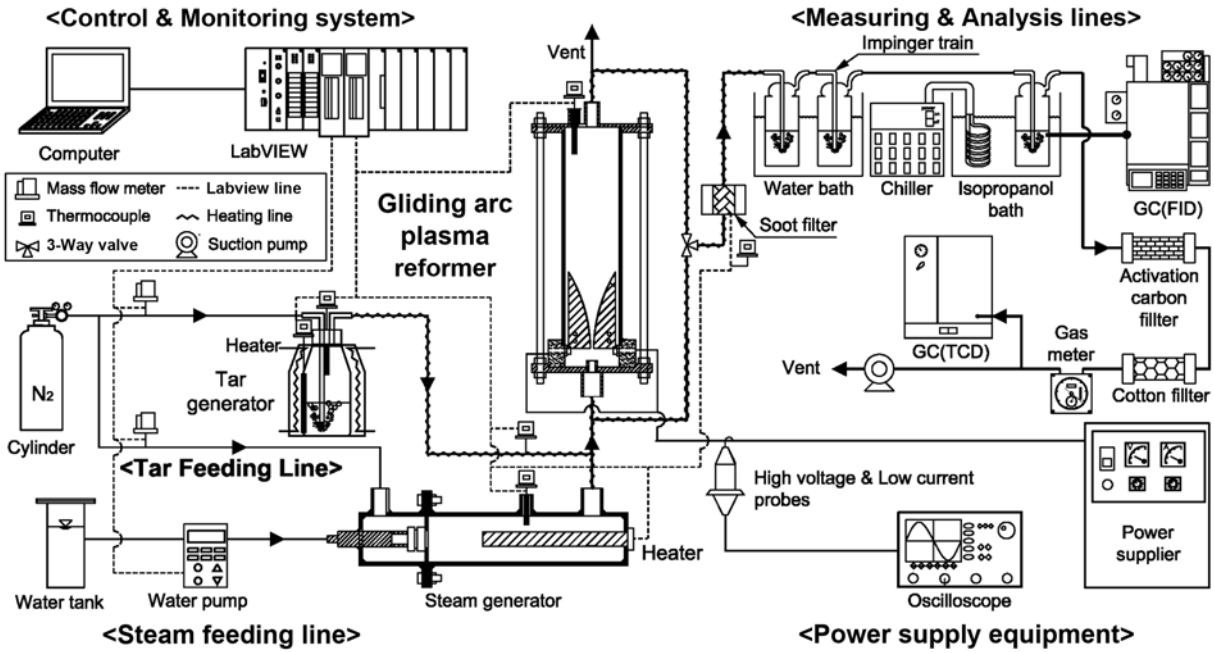

Fig. 2. Experimental setup of the plasma reformer system.

Tektronix, USA) for electrical-characteristic measurement. The power supply provided three-phase AC current up to 15 kW power (voltage: 15 kV; AC current: 1 A) to the gliding arc plasma. The power was measured with the voltage and current probe.

The measurement and analysis line consisted of a sampling device and an analysis device. The sampling device consisted of a soot filter (LS-25 model, Advantec, Japan), an impinger, and a thermostatic bath and chiller (ECS-30SS model, Eyela Co., Japan). The analysis device consisted of a GC-FID for tar analysis (GC-14B model, SHIMADZU, Japan) and a GC-TCD for gas analysis (CP-4900 model, Varian, Netherlands). The MFC, water pump, and heater were connected to the LabVIEW (LabVIEW 8.6 model, National Instrument, USA) control and monitoring system and were controlled by a computer. The temperature, steam flow rate, and nitrogen gas flow rate were continuously monitored.

2. Experiment Method

Fig. 3 displays the initial operation characteristics and stabilization condition for each part in the experimental test rig. The testes were achieved after stabilizing the temperatures at each part.

The accuracy of the tar generation concentration is determined by injection dilution gas (N_2) and vapor pressure depending on the temperature in the tar generator. The temperature of the tar generator was maintained at 260 °C between melting point (218 °C) and boiling point (340 °C) for anthracene. N_2 was fed to the liquid tar in the generator to evaporate precisely by controlling MFC thus producing the required anthracene-concentration (0.1-0.68 g/Nm^3).

To protect line condensation of anthracene, the temperatures of tar feeding line and sampling line were maintained as follows: the tar feeding line between the tar generator and the reformer was maintained at 400 °C. The sampling line between the reformer and the water bath was kept at 150 °C. The soot filter was kept at 120 °C. Temperature of a steam generator was set to about 500 °C.

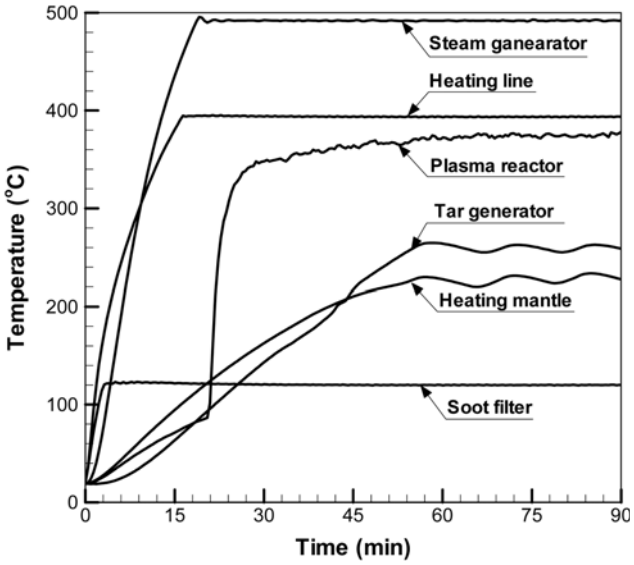

Fig. 3. Initial operating conditions.

At this state, nitrogen of 0.05 L/min into a tar generator and nitrogen of 12 L/min into a steam generator were introduced. Both gases were mixed after the steam generator, and entered into the plasma reformer. At the same time, discharge was formed at the gliding arc plasma reformer.

Table 1 shows the test conditions and the reference values for the variables.

2-1. Sample Analysis Method of Tar, Carbon Black, and Gas

The wet-type sampling method, which was used for tar sampling [13], was conducted at the inlet and outlet of the plasma reformer. Three impingers were separately installed in two baths. The temperature of the first water bath was kept constant at 20 °C or below, and two impingers filled with 50 mL isopropanol were installed. The temperature of the second isopropanol bath was kept constant at −20 °C or below using a chiller, and an empty impinger was installed.

The tar in the gas was condensed and collected in the impingers in the two baths. A suction pump (N-820.3FT 18 model, KNF, Switzerland) was used for the collection of tar and steam at a flow rate of 3 L/min for 20 min.

The tar solution that was collected in the impinger was analyzed by using the GC-FID. An RTX-5 column (RESTEK, USA; 30 m-0.53 mm id; 0.5 μm film thickness) was used for the tar analysis. The oven temperature was kept constant at 45 °C for 2 min, and was increased at a rate of 7 °C/min to 320 °C, which was maintained for 2 min. The temperatures of the detector and injector were set at 340 and 250 °C, respectively.

The sampling of carbon black and gas was conducted along with the tar sampling at the plasma reformer outlet. The carbon black was collected at the soot filter using a glass filtering paper (GA-100 model, Advantec, Japan). The weight of the collected carbon black was determined by comparing its weights before and after the sampling. The concentration was expressed in the collected carbon weight divided by the amount of gas flow. The gas that passed through the impinger was analyzed by the GC-TCD after going through the cotton and activated carbon filters. The two filters were installed to prevent the remaining tar from entering the GC. In the gas analysis from the column, H_2, CO, CH_4, O_2, and N_2 were analyzed using MolSieve 5A PLOT, and CO_2, C_2H_4, and C_2H_6 were analyzed with PoraPLOT Q.

2-2. Error Analysis

Table 2 shows the calibrated range, accuracy and relative error of equipment. Errors in experiments can arise from instrument conditions, calibration, observation and test planning. The accuracy of the experiments was proved with an error analysis.

After this, each data analyzed the polynomial regression. Polynomial regression was calculated using Eq. (1). The standard devia-

Table 1. Experimental parametric-range and reference conditions

Experimental conditions	Steam flow rate (L/min)	Specific energy input (kWh/m^3)	Total gas flow rate (L/min)	Input tar concentration (g/Nm^3)
Range	0-1.57	0.175-0.234	7.2-30.1	0.1-0.68
Reference case	0.37	0.175	12.05	0.27

Table 2. The calibrated range, accuracy and relative error of measurement

Measurement	Equipment	Calibrated range	Accuracy	Relative error (%)
Gas chromatography (Tar; Anthracene)	Shimadzu, GC-14B	100 ppm-100%	±2.5%	<0.5
Gas chromatography (Gases)	Varian, MicroGC-4900	1 ppm-100%	±2%	<0.5
Temperature	K-type (D: Ø 0.3)	273-1643 K	±1 K	±0.25
Mass flow meter (Dilution N_2)	Bronkhost, F201AC-FAC-22-V	0-20 L/min	±1%	±0.25
Mass flow meter (Tar gas generation N_2)	Line Tech, M3030V	0-1 L/min	±1%	±0.25
Gas meter	Sinagawa DC-2A	10-2,000 L/hr	±1%	<0.5
Electronic balance	Shenyang longteng HS-250D	0-180 g	±0.00001 g	±0.1
High voltage	Tektronix, P6015A	1.5-20 kV	±1 V	±0.005
Current	Tektronix, A6303	0-40 A	±5 mA	±0.01

Table 3. The standard errors of maximum values

	Decomposition efficiency	Energy efficiency	Carbon black	H_2	CO	CO_2	CH_4	C_2H_4	C_2H_6
Values (%)	1.28	0.49	0.01	0.03	0.01	0.01	0.001	0.003	0.002

tion (SD) and standard error (SE) were calculated using Eqs. (2) and (3) [18].

$$y=a_0+a_1x+a_2x^2 \quad (1)$$

$$SD=\sqrt{\frac{\sum_{i=1}^{n}(y-y')^2}{n-1}} \quad (2)$$

$$SE=\frac{SD}{\sqrt{n}} \quad (3)$$

In the present study, each experiment was performed two or three times at each experimental condition. Table 3 shows the standard errors of maximum values.

2-3. Data Analysis

The tar decomposition efficiency, energy efficiency, specific energy input, and carbon balance of the gliding arc plasma reactor were calculated from Eqs. (4)-(7).

Eq. (4) shows the tar decomposition efficiency.

$$\eta_t(\%)=\frac{[TC]_{inlet}-[TC]_{outlet}}{[TC]_{inlet}}\times 100 \quad (4)$$

Where $[TC]_{inlet}$ is the input tar concentration (g/Nm^3) and $[TC]_{outlet}$ is the tar concentration at the outlet after the plasma reaction.

Eq. (5) shows the energy efficiency.

$$\eta_e(\text{g/kWh})=\frac{[TC]_{removal}\times Q}{IP} \quad (5)$$

Where $[Tar]_{removal}$ is the removed-tar concentration (g/Nm^3), Q is the amount of gas fed into the reactor (m^3/hr), and IP is the plasma input power (kW).

Eq. (6) shows the specific energy input (SEI).

$$SEI\ (\text{kWh/m}^3)=\frac{IP}{Q} \quad (6)$$

Eq. (7) shows the carbon balance.

$$\text{Carbon balance}\ (\%)=\frac{[CO]+[CO_2]+[CH_4]+2[C_2H_4]+2[C_2H_6]+CB}{A([TC]_{inlet}-[TC]_{outlet})}\times 100 \quad (7)$$

Where [CO], $[CO_2]$, $[CH_4]$, $[C_2H_4]$, and $[C_2H_6]$ are the concentrations of each ingredient (g/Nm^3), CB is the carbon black concentration (g/Nm^3), and A is the carbon constant, which is the number of carbon atom (i.e., 14 for anthracene).

RESULTS AND DISCUSSION

A gliding arc plasma reformer was developed to remove tar from the pyrolysis gas produced from biomass or waste. Anthracene was selected as the tar compound and was tested according to the con-

Table 4. Optimal conditions and their results

Optimum case				
Conditions	Steam flow rate (L/min)	Specific energy input (kWh/m^3)	Total gas flow rate (L/min)	Input tar concentration (g/Nm^3)
Value	0.63	0.175	12.05	0.21

Experiment results											
Result	Gas composition after the reformer (%, N_2 excluded)						Carbon black (g/Nm^3)	Carbon balance (%)	Higher heating value (kJ/Nm^3)	Decomposition efficiency (%)	Energy efficiency (g/kWh)
	H_2	CO	CO_2	CH_4	C_2H_4	C_2H_6					
	79.2	9.5	11.3	0	0	0	0	98.0	11,324	96.1	1.14

Table 5. Comparison between different light tar plasma reforming techniques

	Yu et al. [12]	Tippayawong et al. [19]	Du et al. [20]	This work
Plasma discharge type	DC gliding arc	AC gliding arc	AC gliding arc	3 Phase AC gliding arc
Light tar model	Naphthalene	Naphthalene	Toluene	Anthracene
Input concentration (g/m^3)	1.32	0.13	7.85	0.21
SEI (kWh/m^3)	0.4686	1	0.26	0.175
Decomposition efficiency (%)	92.3	95	98.5	96.1
Energy efficiency (g/kWh)	3.6	0.123	29.46	1.14

ditions of the variables.

Table 4 shows the optimal operating conditions and results. At the optimal conditions, the anthracene decomposition efficiency was 96.1%, and the energy efficiency was 1.14 g/kWh. When the gas was produced according to the anthracene decomposition, the higher heating value was 11,324 kJ/Nm^3. The carbon balance was 98%. It seems that the value of the carbon balance did not reach 100% because some of the deposited and created carbon black was converted into HCN in the reactor [12].

The CH radicals which are produced by ring cleavage in tars and in some intermediates, forms the HCN and CN radical.

$$CH+N_2 \rightarrow HCN+N \quad (8)$$

$$CH+N \rightarrow CN+H \quad (9)$$

A comparison of the results in other researches and this work at reference case is shown in Table 5. The decomposition efficiency and energy efficiency should be affecting the plasma discharge type, model tar and input concentration.

The decomposition efficiency in this work was better than other results, except that Du et al. [20] used toluene (1 benzene ring) which is easier than anthracene (3 benzene rings).

Energy efficiency should be mainly affecting tar removal, which has high value at large input concentration. That is why the energy efficiency of this work showed lower than Yu et al. [12] and Du et al. [20]. However, the value had almost same in case of Tippayawong et al. [18] being lower input concentration like this work.

This work used anthracene with lower input concentration, which is a harder situation than other researches. However, the results of this work are better due to using 3 phase AC gliding arc plasma.

1. Steam Flow Rate Change

Fig. 4 shows the results according to change in the steam flow rate with the total gas flow rate of 12.05 L/min and the SEI of 0.17 kWh/m^3. When the steam flow rate exceeded 1.57 L/min, the temperature of the steam generator started to decrease. Therefore, the testing range was determined to be 0-1.57 L/min.

The decomposition efficiency was 61% at without steam feed (i.e., the steam flow rate of 0 L/min). The decomposition efficiency increased with the increase in the steam flow rate, and it reached 96.1% at the steam flow rate of 0.63 L/min. Then the decomposition decreased with the increase in the steam flow rate.

When steam was not fed, the cracking reaction (Eq. (10)) decomposed tar to create hydrocarbon and hydrogen. In addition, the tar generated carbon black and hydrogen according to Eq. (11) [19].

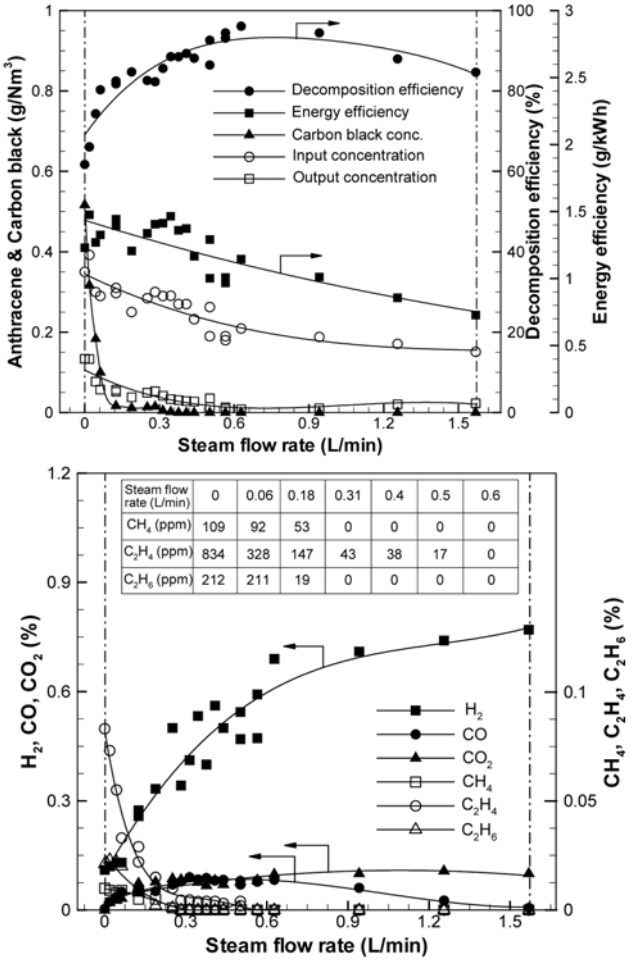

Fig. 4. Effect of the various steam flow rates.

- Formation of carbon black

$$C_nH_x \rightarrow nC+(x/2)H_2 \quad (11)$$

Where, C_nH_x represents tar, such as the large molecular compounds, and C_mH_y represents a hydrocarbon with a smaller carbon number compared to that of C_nH_x.

Thereafter, the steam that was fed into the plasma reformer produced OH radicals according to radical production reaction (Eq. (12)). As shown in Eq. (13), the created OH radicals reacted with tar and were converted into other products [11]. Accordingly, the tar decomposition efficiency increased with the steam injection.

- Radical production

$$H_2O+e \rightarrow OH+H+e \quad (12)$$

- Cracking reaction

$$pC_nH_x \rightarrow qC_mH_y+rH_2 \quad (10)$$

- Radical utilization

$$OH+tar \rightarrow Products \quad (13)$$

Temperature in the plasma reformer was 250 °C for cold air plasma. But in the case of hot steam feeding and line heating in this study, the temperature in the reformer was higher than the cold air plasma (e.g., 380 °C at optimal condition). So, the tar destruction might be affected slightly in producing OH radical, reaction rate, etc.

However, the steam amount also has an adverse effect on tar removal due to its electronegative characteristics [20]. Too many water molecules by increase of steam feed amount limits the electron density in the reformer and quenches the activated chemical species. That is why the decomposition efficiency decreased after reaching the maximum value.

The energy efficiency decreased gradually with the increase of steam flow rate. Increasing the steam feed amount brings about lower input concentrations so that the removed-tar concentrations in Eq. (5) were decreased. That is why the energy efficiency decreased.

The carbon black concentration was 0.51 g/Nm^3 without steam injection. After the value, it decreased significantly, showing almost zero value at the steam flow rate of 0.37 L/min or more. The carbon black formed by Eq. (11), was decomposed by the reactions (Eqs. (14) and (15)), wherein the carbon black was oxidized to CO, CO_2, and H_2 due to the OH radicals [21].

$$C_x+OH \rightarrow C_{x-1}+CO+1/2H_2 \quad (14)$$

$$C_x+2OH \rightarrow C_{x-1}+CO_2+H_2 \quad (15)$$

The major reformed gases included H_2, CO, and CO_2. Small quantities of methane, ethylene, and ethane were also observed. H_2 continued to increase according to Eqs. (10), (11), (14), and (15), and reached 0.77%. CO increased to 0.09% until the steam flow rate reached 0.63 L/min according to Eq. (14), but it decreased according to steam shifting reaction (Eq. (16)) when the steam flow rate exceeded 0.63 L/min. CO_2 was created according to Eq. (15) and increased slightly according to Eq. (16) [22].

$$CO+H_2O \rightarrow CO_2+H_2 \quad (16)$$

Methane, ethylene, and ethane decreased with the increase in the steam flow rate, and they were not produced at the steam flow rate of 0.5 L/min or more. The tar was decomposed to make hydrocarbon substances according to Eq. (10). With the increase in the steam flow rate, the hydrocarbons were converted into H_2 and CO according the steam-reforming reaction (Eq. (17)) [8].

$$C_nH_m+nH_2O=nCO+(n+m/2)\,H_2 \quad (17)$$

2. Energy Input Change

Fig. 5 shows the effect of the specific energy input (SEI) (see Eq. (3)). The experiments were conducted within the SEI range of 0.175-0.234 kWh/m^3.

With the increase in the SEI, the decomposition efficiency increased gradually. The decomposition efficiency was 88% at a SEI of 0.175 kWh/m^3, and it increased to 94.1% at a SEI of 0.234 kWh/m^3. As the increase of the SEI, the electrons and OH radicals between the electrodes increased. The created electrons and OH radicals became more active due to the increased input electric power [23]. And then the radicals converted tar to product gases (H_2, CO, and CO_2), showing increasing tar destruction.

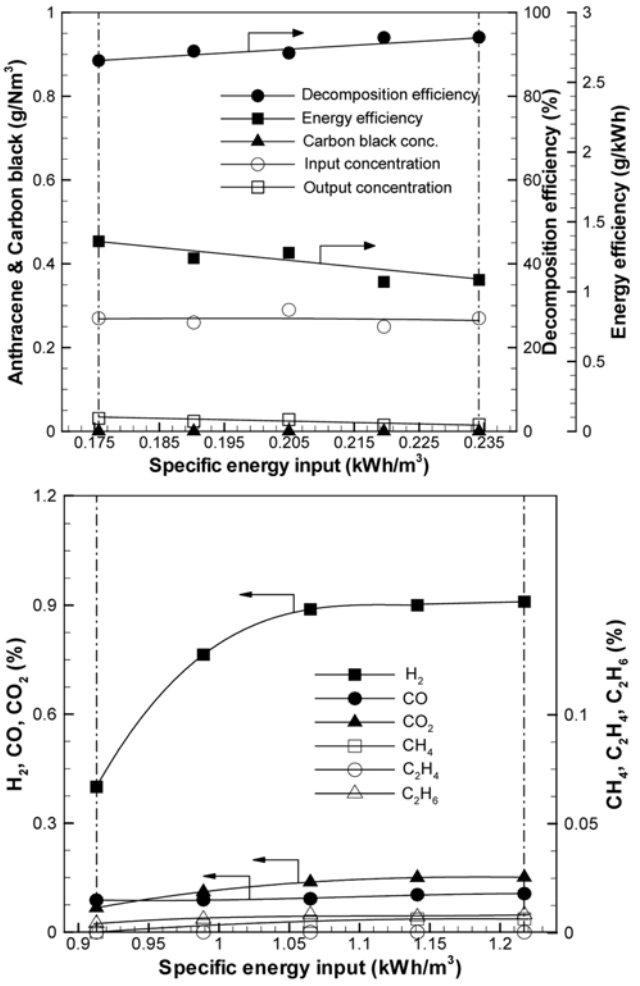

Fig. 5. Effect of the various specific energy inputs.

Carbon black was not collected within the test range because the carbon black converted to producer gases by OH radical as shown in Eqs. (14) and (15).

H_2 increased significantly up to SEI of 0.234 kWh/m^3 according to Eqs. (10), (11) and (14)-(17). CO and CO_2 increased slightly to Eqs. (14)-(17), having lower value than H_2. Hydrocarbons (CH_4, C_2H_4, C_2H_6) increased slightly.

3. Total Gas Flow Rate Change

Fig. 6 shows the total gas flow rate change. The total gas flow rate was controlled and kept within the range of 7.2-30.1 L/min.

The discharge was unstable at a total gas flow rate of 7 L/min or below, because the gas velocity from the nozzle was low. And at a total gas flow rate of 30 L/min or more, the plasma discharge blew off due to high gas velocity. Therefore, the test range was determined to be 7.2-30.1 L/min.

The decomposition efficiency slightly increased and it then had a maximum value of 88.5% at 12.05 L/min due to best plasma discharge. After that value was reached, the efficiency decreased gradually. This tendency is possibly due to the shortening of both contact area and interaction time between anthracene tar and the plasma region, which led to the reductions of energetic electrons impact dissociation and also the reactions between tar and reactive ions

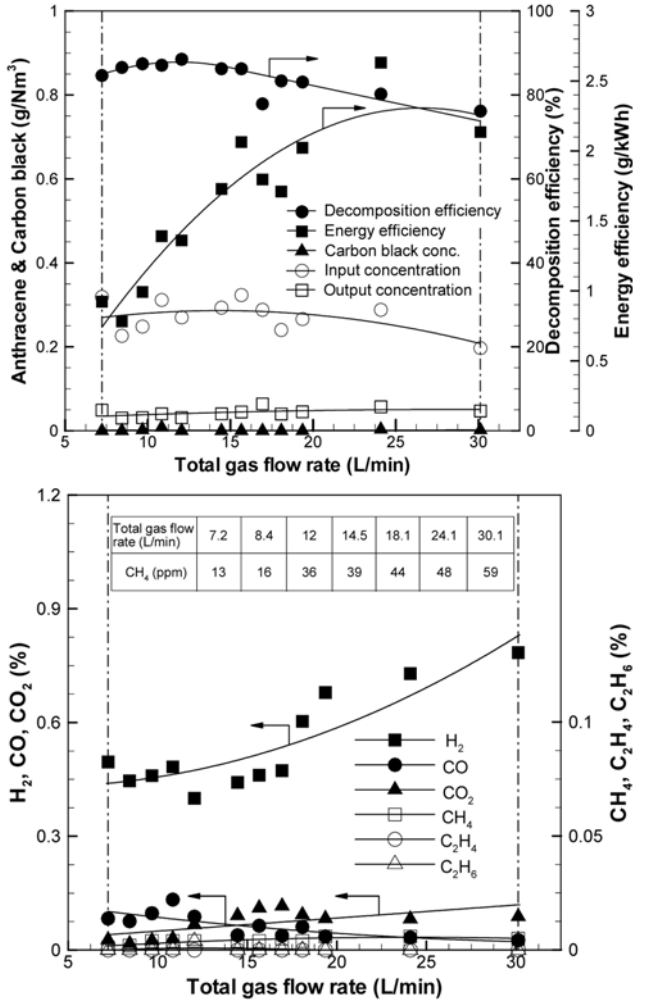

Fig. 6. Effect of the various total gas flow rates.

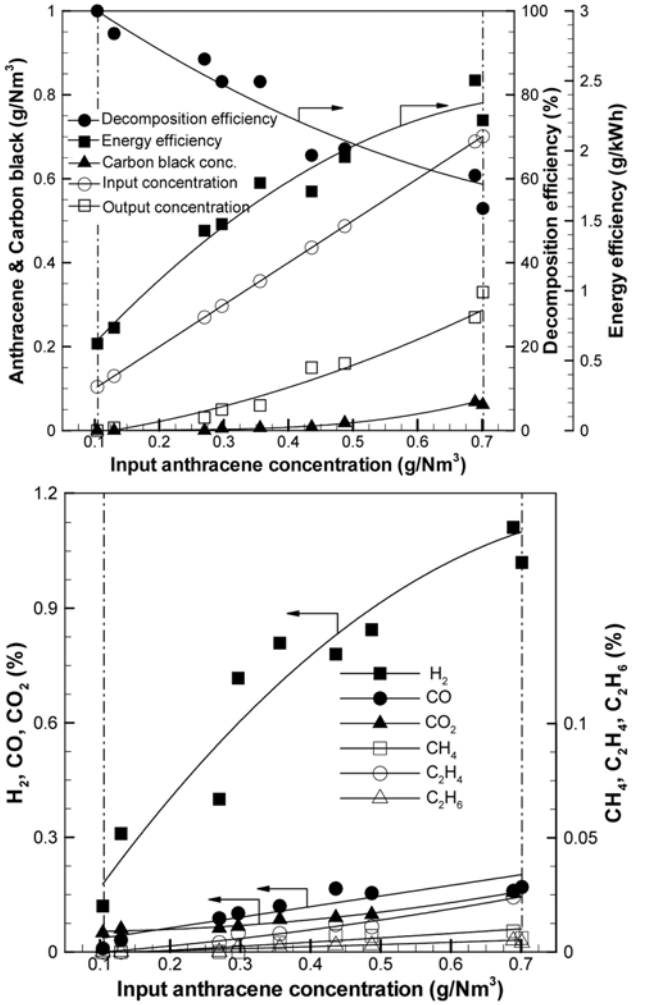

Fig. 7. Effects of the various input anthracene concentrations.

and OH radicals [24].

The energy efficiency increased significantly up to the total gas flow rate of 24 L/min (2.63 g/kWh), having almost constant value after that. This was because the tar removal decreased due to the decrease in the retention time.

The carbon black was not collected by the change of total gas flow rate because the amount of steam feed was fixed as 0.37 L/min. The fed steam creates OH radicals, which can oxidize the generated carbon according to the reactions (Eqs. (14) and (15)).

With increase of total gas amount, H_2 increased gradually. This is because secondary gas reactions (Eqs. (14)-(17)) react significantly with high gas interactions. CO decreased with the increase in the total gas flow rate, while CO_2 increased. The carbon that was produced from the initial cracking reaction was converted into CO according to Eqs. (14), and the produced CO was converted into CO_2 according to Eq. (16). C_2H_4 and C_2H_6 were not generated, but the CH_4 increased with the increase in the total gas flow rate. This is due to the decomposition of C_2H_4 and C_2H_6 to CH_4. Some of the typical reactions are as Eqs. (18) and (19) [25]:

$$C_2H_6 \rightarrow C_2H_4+H_2 \quad (18)$$

$$C_2H_4 \rightarrow CH_4+C \quad (19)$$

4. Input Tar Concentration Change

Fig. 7 shows the effect of the anthracene input concentration. The test was conducted at the initial anthracene concentration of 0.1-0.7 g/Nm^3.

The decomposition efficiency decreased with the increase in the anthracene concentration. Particularly, at an input tar concentration of 0.36 g/Nm^3 or more, the decomposition efficiencies had lower value than about 80%, which cannot be accepted as the reformer. The reason is that the amounts of electrons and active species from the plasma discharge were constant due to the excess of designed capacity in the fixed plasma reformer.

The change in the tar concentration significantly influenced the energy efficiency. The energy efficiency proportionally increased with increasing tar concentration, because the anthracene removal increased whereas the decomposition efficiency decreased.

The carbon black increased slightly at the tar concentration of 0.27 g/Nm^3 or more. The fixed steam amount could not produce enough OH radical to react with anthracene by Eqs. (11) and (12).

With the increase in the anthracene feeding concentration, H_2 increased significantly, while CO, CO_2, CH_4, C_2H_4, and C_2H_6 increased slightly. The amount of increased anthracene gives a conversion to higher light hydrocarbon. The light hydrocarbons react with each

gas according to Eqs. (10), (11) and (14)-(19), respectively. That is because the light gases increased with increasing anthracene concentration.

CONCLUSION

A gliding arc plasma reformer was developed to decompose tar, which is produced from the steam gasification of biomass and waste, and anthracene was used as the representative substance of tar.

At the optimal condition, the anthracene decomposition efficiency was 96.1%, and the energy efficiency was 1.14 g/kWh. The higher heating value of the gas produced from the anthracene decomposition was 11,324 kJ/Nm^3 (except for N_2), and the carbon balance was 87.6%.

The decomposition efficiency was 61% without steam feed. The decomposition efficiency increased with the increase in the steam flow rate, and reached 96.1% at the steam flow rate of 0.63 L/min. Then the decomposition decreased with the increase in the steam flow rate.

With the increase in the SEI, the decomposition efficiency increased gradually. The decomposition efficiency was 88% at a SEI of 0.175 kWh/m^3, and it increased to 94.1% at a SEI of 0.234 kWh/m^3.

The decomposition efficiency slightly increased and then had a maximum value of 88.5% at 12.05 L/min due to best plasma discharge. After reaching that value, the efficiency decreased gradually.

The decomposition efficiency decreased with the increase in the anthracene concentration. Particularly, at the input tar concentration of 0.36 g/Nm^3 or more, the decomposition efficiencies had lower value than about 80% which cannot be accepted as the reformer.

ACKNOWLEDGEMENTS

This research was supported by Basic Science Research Program through a National Research Foundation of Korea (NRF) grant funded by the Ministry of Education, Science, and Technology (2010-0004156).

REFERENCES

1. R. Rauch, H. H. K. Bosch and I. Siefert, *In second world conference and technology exhibition on biomass for energy and industry*, Florence, Italy, 1687 (2004).
2. H. Sutcu, *Korean J. Chem. Eng.*, **24**, 736 (2007).
3. K. Sato and K. Fujimoto, *Catal. Commun.*, **8**, 1697 (2007).
4. L. Devi, K. J. Ptasinski and J. J. G. Janssen, *Ind. Eng. Chem. Res.*, **44**, 9096 (2005).
5. L. Devi, K. Ptasinski, F. Janssen, S. van Paasen, P. Bergman and J. Kiel, *Renew. Energy*, **30**, 565 (2005).
6. K. Zhang, H. T. Li, Z. S. Wu and T. Mi, *2009 International conference on energy and environment technology*, Guilin, China, 655 (2009).
7. L. Fagbemi, L. Khezami and R. Capart, *Appl. Energy*, **69**, 293 (2001).
8. D. Dayton, *National renewable energy laboratory*, NREL/TP-510-32815, 1 (2002).
9. J. Fjellerup, J. Ahrenfeldt, U. Heriksen and B. G. Gobel, *Biomass gasification group*, *DTU*. MEK-ET-2005-05 (2005).
10. C. Li, D. Hirabayashi and K. Suzuki, *Fuel Process. Technol.*, **90**, 790 (2009).
11. A. J. M. Pemen, S. A. Nair, E. J. M. Van Heesch, K. J. Ptasinski and A. A. H. Drinkenburg, *Plasma Sci.*, **8**, 209 (2003).
12. L. Yu, X. Li, T. Xin, W. Yu, L. Shengyong and Y. Jinahua. *J. Phys. Chem. A.*, **114**, 360 (2009).
13. T. Phuphuakrat, T. Namioka and K. Yoshikawa, *Appl. Energy*, **87**, 2203 (2010).
14. A. Czernichowski, *European Roadmap of Process Intensification*, **3.3.5.1**, 18 (2007).
15. A. Czernichowski, M. Czernichowski and K. Wesolowska, *HYPOTHESIS V*, Porto Conte, Italy, September (2003).
16. L. Lin, B.Wu, C. Yang and C. Wu, *Plasma Sci. Technol.*, **8**, 653 (2006).
17. A. Fridman, S. Nester, L. A. Kennedy, A. Saveliev and O. Mutaf-Yardimci, *Prog. Energy Combust. Sci.*, **25**, 211 (1999).
18. D. L. Streiner, *Can. J. Psychiatry*, **41**, 498 (1996).
19. N. Tippayawong and P. Inthasan, *Int. J. Chem. React. Eng.*, **8**, 1 (2010).
20. C. M. Du, J. H. Yan and B. Cheron, *Plasma Sources Sci. Technol.*, **16**, 791 (2007).
21. C. M. Du, J. H. Yan, X. D. Li, B. G. Cheron, X. F. You, Y. Chi, M. J. Ni and K. F. Cen, *Plasma Chem. Plasma Process.*, **26**, 517 (2006).
22. Y. N. Chun, Y. C. Yang and K. Yosikawa, *Catal. Today*, **148**, 283 (2009).
23. T. Sreethawong, P. Thakonpatthanakun and S. Chavadej, *Int. J. Hydrog. Energy*, **32**, 1067 (2007).
24. Z. Bo, J. Yan, X. Li, Y. Chi and Kefa Cen, *J. Hazard. Mater.*, **155**, 494 (2008).
25. B. Zhang, S. Xiong, B. Xiao, D. Yu and X. Jia, *Int. J. Hydrog. Energy*, **36**, 355 (2011).